A Bio-inspired Distributed Approach for Searching Underwater Acoustic Source using a team of AUVs

Mansoor Shaukat*, Mandar Chitre† and Sim Heng Ong‡
*NUS Graduate School for Integrative Sciences & Engineering, National University of Singapore, Singapore, 117456
Email: mansoor@arl.nus.edu.sg
†Acoustics Research Lab, Tropical Marine Science Institute and
Department of Electrical & Computer Engineering, National University of Singapore, Singapore, 119222
Email: mandar@arl.nus.edu.sg
‡Department of Bioengineering and
Department of Electrical & Computer Engineering, National University of Singapore, Singapore 117583
Email: eleongsh@nus.edu.sg

***Abstract*—We present a bio-inspired distributed algorithm which is a fusion of two distinct animal behaviours to solve three different underwater search missions. One of the two constituent control modules is called *target-drive* which models the hypothesized behaviour of a fish-larva searching for a coral reef using acoustic cues. Target-drive helps a single Autonomous Underwater Vehicle (AUV) to adjust its heading towards the acoustic source. The other control module called *group-cohesion*, mimics movements of a golden shiner (Notemigonus crysoleucas) in a school of fish. The proposed approach only relies on *implicit* communication and achieves target convergence only by assuming a single on-board hydrophone and location estimate of AUV's neighbours. The effects of varying key parameters such as group-size and neighbourhood-radius on convergence times have been thoroughly investigated. We present a preliminary analysis of the algorithm's performance which shows promise in solving problems employing *small teams* of AUVs in terms of convergence times and non-existent inter-agent communication.**

I. Introduction

An AUV can undertake diverse engineering endeavours such as oceanographic surveys [1], monitoring marine environments [2]–[3], reconnaissance/surveillance missions [4] and offshore exploration [5]. Efficiency of conducting such tasks can be enhanced if a team of AUVs is deployed [6]–[7]. A conventional team-based scenario requires flow of information between surface vehicles/buoys and the AUVs [8]. The multitude of sensors installed on each of the surface and underwater vehicles are capable of measuring various physical parameters, and hence synchronizing this vast information in a centralized network becomes unviable. This is further aggravated if we consider acoustic communication to be the only mode of long-range underwater communication [9]. For a communication system designer, an underwater acoustic channel presents its fair share of challenges [10]–[11]. Issues like propagation delay, time varying multi-path fading and frequency-dependent path-loss further complicates the design of a long-distance underwater communication system [8],[12]–[13]. Conventional methods of underwater acoustic communication are more focussed on achieving robustness and higher data rates but do not scale well with increasing number of agents [14].

Today, in the world of robotics, there is an increasing interest in swarms where a *swarm* can be defined as a *large* team of entities interacting *locally* with common goals [15]. Question is often raised pertaining to the need of a robotic swarm where a single robot is sufficient to complete a task. This question can be effectively answered by highlighting some of the advantages associated with a team of robots. Firstly, a team can swiftly find targets and areas of interest [16]–[18], and supports superior situational awareness, entry and exit strategy [19]. Secondly, an agent break-down in a single robot/AUV mission implies mission failure but a large team is robust towards multiple failures [18]–[22]. Moreover, workload distribution within a team results in more efficient solutions [23]–[24]. Finally, a team can carry out a large number of tasks in parallel with simpler and cheaper agents [23].

However, it is important to note that in case of AUVs where cost plays an important role, only smaller teams may be feasible [25]. This fact underscores the need of a distributed algorithm which can not only exploit deployment of a large team but is also able to show significant benefits in recruiting a smaller team (10 or 20 AUVs). In this work, our focus is to search for an underwater acoustic source with such a small team of AUVs.

To harness the benefits of a team with minimal inter-agent communication owing to the intricacies of an underwater communication channel as discussed earlier, one could look towards nature. Nature has been choreographing complex patterns in huge swarms by relying on *implicit* communication [26]–[31]. At this point, it is imperative to differentiate clearly between implicit and explicit communication. Explicit communication is defined as a *deliberate act of invoking the signal transmission*, whereas in implicit communication there is no such deliberate attempt [32]. In the latter, the information transfer happens passively, without the need to actively transmit information to another agent. For example, an agent may simply observe the behaviour of other agents using its own sensors. Complex behaviour displayed by natural swarms arises from simple individual rules [33]. Individuals in a swarm do not require any knowledge of an overall pattern and only based on local interactions, they generate very complex emergent behaviour which is greater than the sum of its parts.

Following nature's awe-inspiring displays, researchers especially in the field of robotics have tried to mimic nature. A significant number of practical implementations on mobile robots draw inspiration from emergent behaviours of termites or ants. These behaviours primarily use pheromone deposited in the environment by their peers as the primary mode of communication [34]–[37]. Relevant implementations to search based tasks are those of finding chemical sources. Mobile robots can successfully detect a chemical source, mimicking the behaviour of a male moth searching for a female moth with the aid of her pheromone trail [38]–[39]. There are also accounts of an AUV finding chemical source by plume tracing [40]–[41]. However, multi-AUV implementations of such approaches are only a scaled version of a single agent case [42] or require explicit inter-agent communication to coordinate a search mission [43]–[44].

Other than the bio-inspired algorithms, there are other relevant source detection implementations as well. Single-agent based extremum seeking search solutions have been proposed which employ gradient-based methods for point mass or non-holonomic vehicles having a single onboard sensor [45]–[46]. In case of underwater acoustic localization, *vehicle homing* for AUVs bears some relevance to our proposed work [47]–[49]. Such solutions, though generic in nature, differ from our proposed solution primarily in terms of the underlying multi-agent problem. Our focus is to search for an underwater acoustic source by exploiting benefits of group cohesion in a small team. Although this text assumes an acoustic source to be the target of interest, the concept is easily extendible to localizing any source characterized by some other physical variable.

We formally present the problem statement with regards to three distinct scenarios in Section II with associated assumptions and physical constraints. In Section III, we define the distributed algorithm with focus on its two constituent bio-inspired models. After defining the algorithm parameters we discuss the results in Section IV, establishing variation in convergence times (arrival at target location) as a function of group-size and neighbourhood-radius. We conclude by summarizing the findings in Section V and discuss our future direction in Section VI.

II. PROBLEM STATEMENT

A. The three scenarios

We define three distinct underwater scenarios which stipulate different requirements for a search mission to be considered as successful. These scenarios will be used to gauge performance of the algorithm and will help differentiate what kind of behaviour is best suited to each one of these. The scenarios are:

1) First arrival problem: Following the unfortunate event of an aircraft crashing into the sea, the lost black-box needs to be found. The black-box is continuously emitting an acoustic pulse which can be sensed within a certain range. A team of Underwater Autonomous Vehicles (AUVs) needs to search for the black-box and the *first* AUV among the group to find the black-box will result in the mission being a success.

2) Specific arrival problem: We now suppose that the black-box, not only has to be discovered but also retrieved to a safe location. For this purpose, there is a specialized AUV within the team with the desired payload capacity to undertake the retrieval task. In this case, as soon as this *specific* AUV arrives at the black-box location, the mission can be considered a success.

3) Last arrival problem: An underwater charging bay, incorporated with a single beacon has been installed at an unknown location. A team of AUVs needs to find the charging bay before each of their batteries run out. As soon as *all* the AUVs reach the charging bay, the mission is said to be accomplished.

B. Assumptions & constraints

For the three scenarios as discussed, we make the following assumptions:

1) Group size and initialization: The group/team size is constrained to that of a small team (5 to 30 agents) and is constant during a particular mission for establishing meaningful comparisons. The team is initialized 2 km away from the acoustic source.

2) Sensing scheme for source localization: All the AUVs in the team are assumed to be equipped with a single hydrophone, able to estimate acoustic intensity to an accuracy of 1 dB. We also assume that there is no estimate available to an AUV pertaining to the direction of incoming sound.

3) Acquisition of neighbours' position estimates: In this paper, we do not address the question of how an AUV acquires the position information of its neighbours. For now, any arbitrary mechanism, e.g., communication of position estimates within a neighbourhood or Ultra Short Base Line (USBL) can be assumed for that purpose. Further simplification of this position estimation model is focus of our future work which will allow us to use a simple 2-hydrophone array as a mechanism to estimate positions of neighbour AUVs.

4) AUV model: All the AUVs have been considered as point masses and physical constraints like turning rates and undersea hydrodynamics do not apply.

5) Source's acoustic level and ambient noise: For the purposes of the simulation results presented in this paper, the sound level for the acoustic source is set to 156 dB re 1μPa at 1m. The ambient noise is set to 123 dB re 1μPa.

III. METHODOLOGY

We consider a team of N AUVs assigned with a search mission. The *target* is the acoustic source as described in Section II-A. In this section, we formulate a novel bio-inspired algorithm that is a result of fusing two natural behaviours. The first module, named *target-drive*, draws its inspiration from fish larvae or juvenile fish searching for the coral reef by sensing the acoustic intensity of noise generated by fish and crustaceans that live on the coral reef [50]–[52] . The second module, named *group-cohesion*, draws inspiration from the group behaviour of schooling fish (golden shiners) [33],[53]. We start by formulating each of these modules and then fuse them together into a unified distributed algorithm.

A. Target-drive

Target-drive is responsible for driving any arbitrary AUV $n \in \{1, 2, \dots, N\}$ towards the acoustic source. $P_n(t)$ is the received mean square pressure at the n^{th} AUV position ${}^0\mathbf{p}_n(t) = [{}^0x_n(t), {}^0y_n(t)]^T$ in a two-dimensional world reference frame $\{0\}$. The origin of $\{0\}$, without loss of generality, is assumed to be fixed at the source's origin and is unknown to any of the AUVs.

The received mean square pressure $P_n(t)$ at point ${}^0\mathbf{p}_n(t)$ is given by:

$$P_n(t) = \frac{P_{source}}{\|{}^0\mathbf{p}_n(t)\|^{\alpha}} + P_{ambient} \tag{1}$$

where $P_{ambient}$ is the mean square ambient noise and $\alpha \in [1, 2]$ approximates anywhere from cylindrical to spherical spreading. For most of the results, discussed in Section IV, we will assume $\alpha = 1$ for maintaining consistency and ease of interpretation. $\alpha > 1$ is assumed in Section IV-E while summarizing results to substantiate generalization.

If we assume the ambient noise to be Gaussian then each sample of received pressure is also Gaussian with variance $P_n(t)$. Let x_i be the received pressure at index i of a time window of k samples over which the mean square pressure $P_n(t)$ is computed. Then, $\sum_{i=1}^{k} \frac{x_i^2}{P_n(t)}$ is χ_k^2 distributed with k degrees of freedom. When $k \to \infty$, $\chi_k^2 \to \mathcal{N}(k, 2k)$. Following this, we can approximate estimated mean square pressure as

$$\hat{P}_n(t) = \lim_{k\to\infty} \frac{1}{k} \sum_{i=1}^{k} x_i^2 \sim \mathcal{N}\left(P_n(t), \frac{2P_n(t)}{k}\right) \tag{2}$$

The variance of this distribution varies with mean $P_n(t)$ and measurement mechanism (effective k). In this case, the mean can be assumed to be much larger than the variance because of k being very large, the asymmetry due to log operation applied on (2) is small and hence the dB levels can be modelled as Gaussian. Since the sensation of loudness is known to be logarithmic in most animals, we assume a constant '$a = 1$dB' of measurement accuracy such that

$$\hat{P}_{n_{dB}}(t) = 10\log_{10}\hat{P}_n(t) \sim \mathcal{N}(P_{n_{dB}}(t), a) \tag{3}$$

The assumed value of a is also true for a typically calibrated hydrophone. The Normal distribution as characterized by (3) simulates the sound levels sensed by an AUV hydrophone at any sampling instant t.

It is assumed that an AUV samples intensity level every T seconds and maintains a constant speed $s(t) = 1.5$m/s, $\forall t$ and a constant heading angle $\theta_n(t)$ during interval $(t, t+T]$. The AUV heading is updated at each sample employing a *90-degree rule* as

$$\theta_n(t+T) = \begin{cases} \theta_n(t) & \text{if } \Delta\hat{P}_{n_{dB}}(t+T) \geq 0 \\ \theta_n(t) + \frac{\pi}{2} & \text{if } \Delta\hat{P}_{n_{dB}}(t+T) < 0 \end{cases} \tag{4}$$

where $\Delta\hat{P}_{n_{dB}}(t+T) = \hat{P}_{n_{dB}}(t+T) - \hat{P}_{n_{dB}}(t)$.

In essence, target-drive is a complete algorithm which drives any AUV towards the target location based only on the gradient of the sensed sound level $\Delta\hat{P}_{n_{dB}}(t+T)$. The 90-degree rule draws its inspiration from the hypothesized motions, a fish larva would undertake to locate the coral reef based on sensed sound levels. There is no agreement on the actual rules a larva follows but there are similar studies with different models to mimic its behaviour [51]. As migrations generally occur under low light or no-light conditions, a larva uses its hearing as a primary sense to locate the coral reef other than using chemical cues [54]. Analogously in AUVs, if the n^{th} agent after a sampling time T *thinks* that it is going in the direction of increasing reef sound, it keeps its direction otherwise it takes a 90-degree turn. This continues until the AUV converges on to the target position. The algorithm on its own does not guarantee convergence and the results depend significantly on the right choice of sampling time T. Though convergence is not guaranteed, we can still stochastically predict arrival times for AUV(s) and their dependence on the group size. However, it has been found in simulations that convergence occurs up to some threshold of difference between P_{source} and $P_{ambient}$ and not beyond that. Mathematical explanation of this observation is focus of our future work. It is also to be noted that a 90-degree turning approach may seem sub-optimal as far as the case for a single agent is concerned but it generates viable convergence times for the team, especially when fused with the group-cohesion behaviour. The efficacy of the target-drive algorithm with respect to the three scenarios will be discussed in detail in Section IV.

B. Group-cohesion

It is believed that group behaviour in a school of fish is based on long-range attraction and short-range repulsion [33],[51]. However, there have been fewer studies on inferring rules directly from the empirical data. A recent study [53] has come up with a novel and intuitive idea of estimating forces generated by golden shiners, based on respective distances from their neighbours in order to maintain cohesion. The study has concluded that there are no independent alignment forces but only a speeding force ${}^nf_x(t)$ and a turning force ${}^nf_y(t)$. These forces depend, respectively on the horizontal and the vertical distance of the n^{th} fish from its neighbour k_1 in its own reference frame $\{n\}$, as shown in Fig. 1. However, it is to be noted that we implement a simplified model of the said study and hence the term *force* carries a slightly different meaning in our work. We impose a constant velocity constraint and only the heading of the AUV is computed from the force vector. This simplification is justified because of the assumed constraints on the AUV model as given in Section II-B.

We model the speeding force and the turning force as linear attractive forces as

$${}^nf_x(t) = -\zeta\ {}^nx(t) \tag{5}$$

$${}^nf_y(t) = -\zeta\ {}^ny(t) \tag{6}$$

where $\zeta \in \mathbb{R}^+$ is the attraction parameter. ζ can be tuned beforehand to achieve the desired strength in group cohesion but remains constant during a mission.

Results in (5) and (6) can be expanded as shown in Fig. 2 to multiple neighbours by averaging respective horizontal and

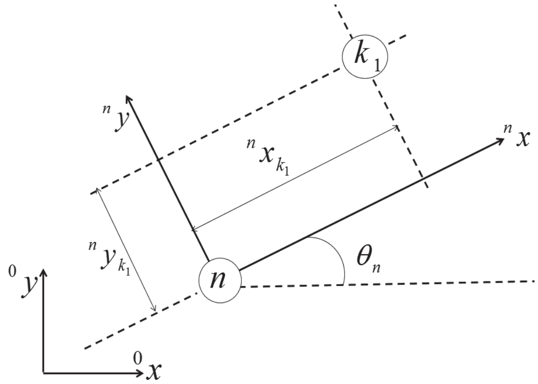

Fig. 1: Calculation of speeding force $^n f_x(t)$ and the turning force $^n f_y(t)$ by n^{th} fish with respect to the horizontal $^n x(t)$, and vertical distance $^n y(t)$ respectively in its own reference frame $\{n\}$.

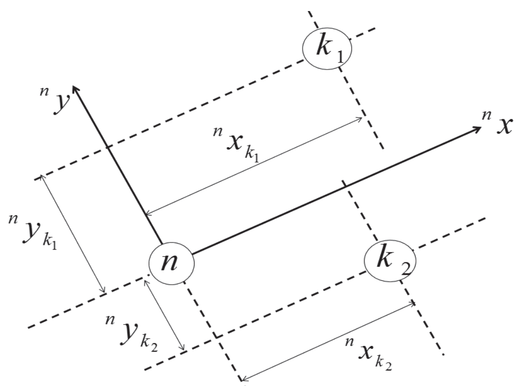

Fig. 2: Calculation of speeding force $^n f_x(t)$ and the turning force $^n f_y(t)$ by n^{th} fish with respect to multiple neighbours.

vertical distances as follows

$$^n f_x(t) = -\frac{\zeta}{M(t)} \sum_{i=1}^{M(t)} {}^n x_{k_i}(t) \tag{7}$$

$$^n f_y(t) = -\frac{\zeta}{M(t)} \sum_{i=1}^{M(t)} {}^n y_{k_i}(t) \tag{8}$$

where all the neighbours of the n^{th} AUV are denoted by k_i ; $i \in \{1, 2, \ldots, M(t)\}$ and there are $0 \leq M(t) < N$ neighbours in a neighbourhood $\Psi_n(t) = \{k_1, k_2, \ldots, k_{M(t)}\}$ with constant Euclidean radius $r_\Psi \in \mathbb{R}^+$ measured from origin of the frame $\{n\}$. The origin is the n^{th} AUV itself being considered as a point mass.

The resultant force $^n f(t) = [^n f_x(t), ^n f_y(t)]^T$ gives us the heading $\theta_n(t) = \angle^n f(t)$ while speed remains constant as $s_n(t) = \upsilon$, where $\upsilon \in \mathbb{R}^+$.

C. Fusing Target-drive & Group-cohesion

Once we have the two bio-inspired models in place, it is of interest to fuse them together into a unified search algorithm. As discussed earlier, target-drive is a complete algorithm in itself which can help an AUV find the target. However, group-cohesion only serves to maintain an arbitrary group formation and swiftly falls into an equilibrium where there is no net motion of the group. We would like to investigate the effect of target-drive on such a cohesive group. Then the challenge is to find a unified architecture that can drive the group as a whole towards the target location.

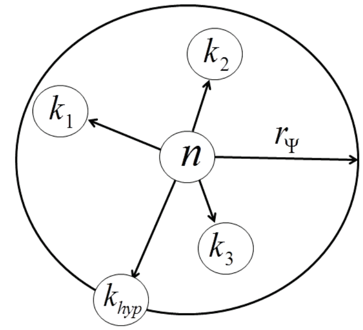

Fig. 3: Introducing a hypothetical neighbour k_{hyp} in the direction of assumed target location among other neighbours k_i of the neighbourhood $\Psi_n(t)$.

For a unified architecture, we modify the group-cohesion algorithm by introducing a hypothetical neighbour k_i as shown in Fig. 3. The hypothetical neighbour bears the same angle with respect to the n^{th} AUV as dictated by $\angle^n f(t)$ as described in Section III-B. The modified group-cohesion model as given in (7)–(8), fused with the target-drive model, looks like

$$^n f(t) = \beta \left(-\frac{\zeta}{M(t)} \sum_{i=1}^{M(t)} {}^n \mathbf{p}_{k_i}(t) \right) + \eta \left(-\zeta \; {}^n \mathbf{p}_{hyp}(t) \right) \tag{9}$$

where $\beta \in \mathbb{R}^+$ is a constant gain of the group cohesion force, called *cohesion-coefficient* and $\eta \in \mathbb{R}^+$ is a constant gain associated with the force that drives a particular AUV towards the target, called *drive-coefficient*. Changing the gains vary the emphasis of the AUVs either towards the target or the group. The effects of these gains will be discussed in detail in Section IV. The unified behaviour in (10) can be more concisely written as

$$^n f(t) = \acute{\beta} \sum_{i=1}^{M(t)} \frac{^n \mathbf{p}_{k_i}(t)}{M(t)} + \acute{\eta} \; {}^n \mathbf{p}_{hyp}(t) \tag{10}$$

where $\acute{\beta} = -\beta\zeta$, $\acute{\eta} = -\eta\zeta$ and $^n \mathbf{p}_{k_i}(t) = [^n x_{k_i(t)}, ^n y_{k_i}(t)]^T$, $^n \mathbf{p}_{hyp}(t) = [^n x_{hyp}(t), ^n y_{hyp}(t)]^T$.

Note that the hypothetical neighbour's position $^n \mathbf{p}_{hyp}(t)$ is being updated according to (4) at every sample time T. From (10), the computation of the n^{th} AUV's heading $\theta_n(t)$ and speed $s_n(t)$ follows the same discussion as presented in Section III-B.

IV. Results & Discussion

We set the starting point of the team at $^0 \mathbf{p}_n(t) = [1414 \text{ m}, 1414 \text{ m}]^T$, 2 km away from the black-box location with the sampling time $T = 66$ s and $\acute{\beta} = 0.5$, $\acute{\eta} = 5$. These

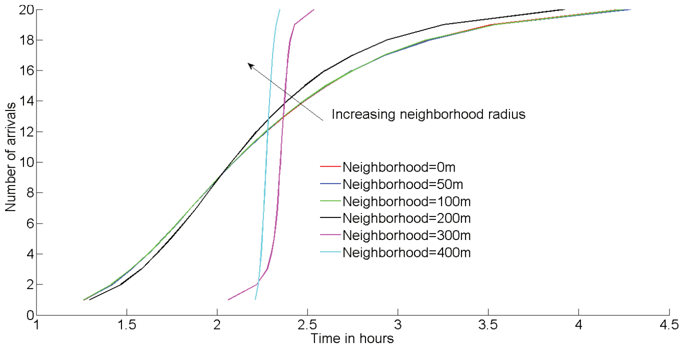

Fig. 4: Average arrival times over 1000 trials for varying neighbourhood sizes r_Ψ for a group-size $N = 20$.

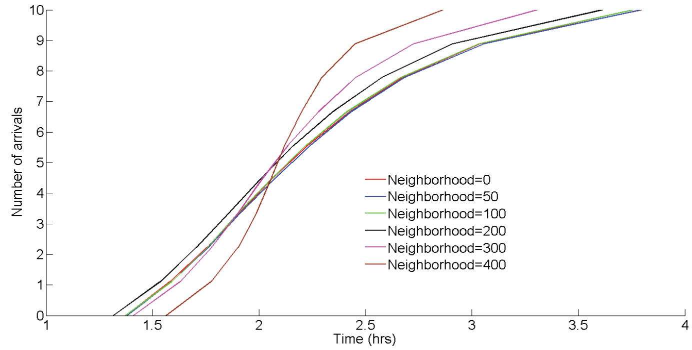

Fig. 6: Average arrival times over 1000 trials for varying neighbourhood sizes r_Ψ for group size $N = 10$.

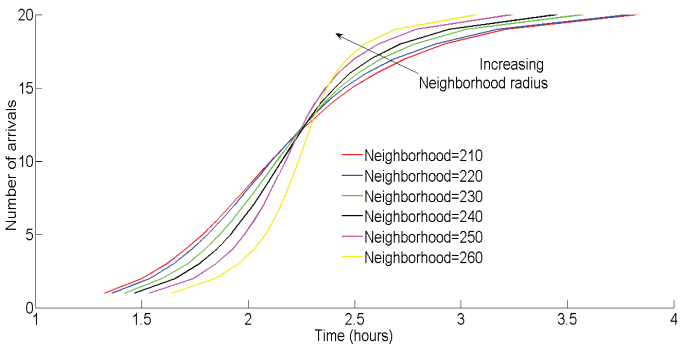

Fig. 5: Average arrival times over 1000 trials for neighbourhood sizes $r_\Psi \in \{210, 220, \ldots, 260\}$ for a group-size $N = 20$.

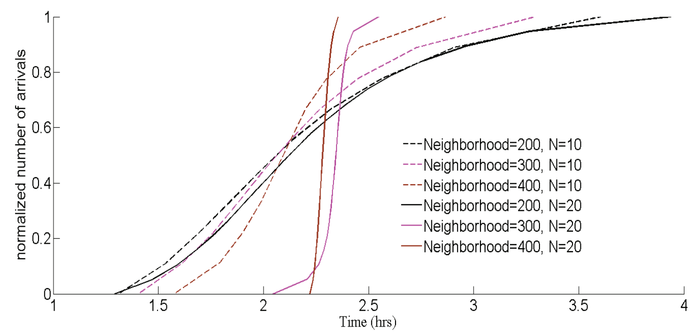

Fig. 7: Average arrival times between group size $N \in \{10, 20\}$ over 1000 trials for neighbourhood sizes $r_\Psi \in \{200, 300, 400\}$.

parameters will remain constant for all the results here and studying their variation effects will be a part of our future work (Section VI). As soon as a an agent enters within a radius $\wp = 100$ m of the target location, we term that as an *arrival*. 1000 independent trials have been run for computation of averages or probabilities as discussed earlier in this section. It is also to be noted that events involving $r_\Psi = 0$ m are a zero-neighbourhood case where there is no group-cohesion involved. In such a case, only target-drive algorithm is active which enables each of the AUVs to take the heading decision based on the sensor reading as given by(3). The speed of the AUV has been assumed to be constant, i.e., $s_n(t) = 1.5$ m/s $\forall t$. The value for $\alpha = 1$ as given in (1) unless otherwise specified.

A. Average arrival times for varying levels of group-cohesion

1) The dead-region $0 < r_\Psi \le \phi_\Psi$: We first simulate a search task involving a team of $N = 20$ AUVs to gauge the effect on the average arrival times over 1000 trials as the neighbourhood radius r_Ψ is varied from 0 m to 400 m as shown in Fig. 4. It can be seen that for a range of neighbourhood radii $r_\Psi = 0$ m to 100 m, the behaviour is almost identical. For $r_\Psi \ge 200$ m the first-arrival on average gets delayed whereas the last-arrival is earlier in time. As there is quite a difference between the arrival times pertaining to neighbourhood radius of 200 m and 300 m, Fig. 5 shows a uniform change for variations in neighbourhood radius from 210 m to 260 m.

To generalize the effect on average arrival times by varying neighbourhood radius, we need to show the same effect on other group sizes as well. Fig. 6 shows the average arrival times for a group size of $N = 10$ AUVs when neighbourhood radius r_Ψ is varied from 0 m to 400 m. The same pattern is seen as was seen for the group size of $N = 20$. There is a similar *dead-region* $0 < r_\Psi \le \phi_\Psi$ of neighbourhood radii, which displays nearly the same behaviour as a zero-neighbourhood. When $r_\Psi = \phi_\Psi$, it is the point where arrival times start varying from that of a zero-neighbourhood region. More intuitively, we can say that ϕ_Ψ is the minimum neighbourhood radius required for the group-cohesion to have any impact on the convergence times. Also, the rate of change in arrival times, as r_Ψ is varied, is not as much as was the case in Fig. 4 for $N = 20$. This means that a larger neighbourhood radius is required in case of $N = 10$ to clock the same average arrival times as was required for $N = 20$. In fact, this can be clearly shown by comparing the effect of neighbourhood variation as shown in Fig. 7. To help us generalize more, we show results for averaged arrivals for a group of $N = 5$ AUVs in Fig. 8 where the response is even flatter than that of $N = 10$.

2) Maximum neighbourhood radius $r_{\Psi_{max}}$: We have mentioned the term *larger* neighbourhood a number of times in the preceding discussion. One may wonder if there is any limit on the neighbourhood radius. The answer is *yes* for two reasons. First, there will always be a physical constraint on the sensing range of a sensor. Secondly, increasing the neighbourhood radius beyond a certain point $r > r_{\Psi_{max}}$ will result in nearly the same averaged last-arrival times as shown in Fig. 9 where $r_{\Psi_{max}} \simeq 800$ m, whereas first-arrival will start occurring in

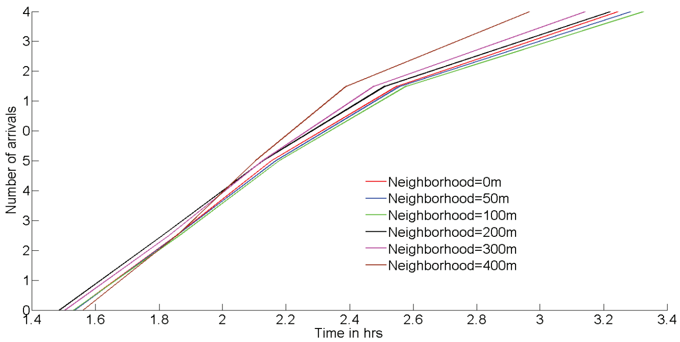

Fig. 8: Average arrival times over 1000 trials for varying neighbourhood sizes r_Ψ for group size $N = 5$.

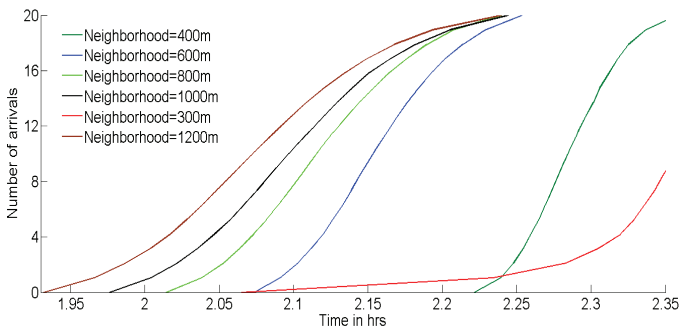

Fig. 9: Average arrival times over 1000 trials for varying neighbourhood sizes r_Ψ for a group-size $N = 20$: Showing the significance of $r_{\Psi_{max}}$.

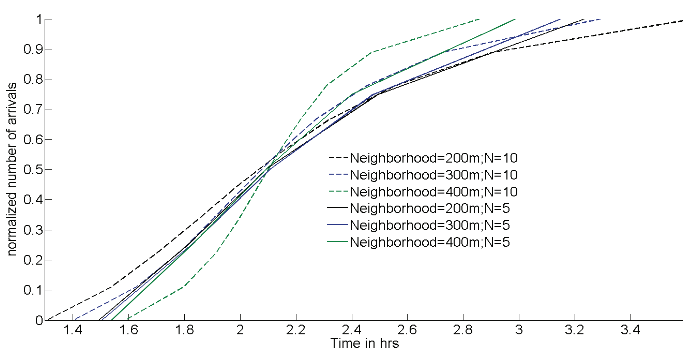

Fig. 10: Comparison of average arrival times between group size $N \in \{5, 10\}$ over 1000 trials for neighbourhood sizes $r_\Psi \in \{200, 300, 400\}$.

a smaller time interval. However, it has to be kept in mind that this first-arrival advantage is not as significant as it was for a zero-neighbourhood case. Hence, we have to be mindful of this upper limit on the neighbourhood radius beyond which there is no significant improvement in arrival times.

3) The transition neighbourhood radius $\acute{r}_\Psi$: One of the interesting things to note is the transition neighbourhood radius $\acute{r}_\Psi$ which acts as a threshold for the decision making process of employing a larger or a smaller group of AUVs. Looking at Fig. 7, it is seen that the advantage of using a larger group, i.e., $N = 20$ is significantly beneficial in terms of averaged last-arrival time only for a neighbourhood radius $r_\Psi \in \{300 \text{ m}, 400 \text{ m}\}$. As r_Ψ is decreased to 200 m, the advantage is swapped in favour of employing a smaller team ($N = 10$). In fact, this holds in general as we compare group sizes of $N = 10$ and $N = 5$ in Fig. 10 where the advantage of using a larger group is valid only for $r_\Psi = 400$ m in terms of averaged last-arrival, and is quite the opposite for $r_\Psi \in \{200 \text{ m}, 300 \text{ m}\}$. Hence, we can say that there exists a transition neighbourhood radius $\acute{r}_\Psi$ which acts as a threshold, above which ($r_\Psi \geq \acute{r}_\Psi$) it is advantageous to use a larger group size to clock smaller last-arrival times whereas this advantage switches to employment of a smaller group below this threshold ($r_\Psi < \acute{r}_\Psi$). It is also to be noted that this critical $\acute{r}_\Psi$ is lower for comparisons between larger group sizes such as $N \in \{10, 20\}$ where it is $\simeq 210$ m whereas $\acute{r}_\Psi$ is higher for comparisons between smaller group sizes such as $N \in \{5, 10\}$ where it happens to be $\simeq 340$ m.

The same discussion holds in an opposite fashion if we would have been talking about averaged first-arrival. The $\acute{r}_\Psi$ shifts the advantage to smaller group sizes once $r_\Psi \geq \acute{r}_\Psi$ and to larger group sizes if $r_\Psi < \acute{r}_\Psi$.

B. *First-arrival times with and without group-cohesion*

The cumulative distribution function (CDF) and probability density function (PDF) for first-arrival times are shown in Fig. 11 and Fig. 12 respectively. It is shown that the event involving the first-arrival for a group size of $N = 20$ AUVs surely occurs before 2 hours had there been no group-cohesion. So in a case such as Scenario 1 in Section II, implementing only the target-drive algorithm would have delivered better results. Though no group-cohesion is required in such a scenario, it is important to note that *group-size* still plays a pivotal role in the first-arrival problem. Increasing the group size increases the chances of having a first-arrival in a shorter span of time. Fig. 13 emphasizes the same point in which we compare a group size of $N = 5$ to $N = 30$. We can establish from these results that scenarios in which only the first-arrival is sufficient to claim mission success; we do not require group-cohesion and only the target-drive algorithm is sufficient. Moreover, better convergence times can be observed if a larger group size is deployed.

C. *Last-arrival times with and without group-cohesion*

If, on the contrary, we were interested in the last-arrival times where the whole group should have reached the target location; the results are quite the opposite to what we have shown for the first-arrival case. For example, as stipulated in Scenario 3 in Section II, we would require each and every AUV to be at the charging bay before the respective batteries run out. A comparison of CDFs and PDFs of last-arrival times for a group size of $N = 20$ has been made between neighbourhood radii $r_\Psi = 0$ m and 300 m in Fig. 14 and Fig. 15 respectively. Then, it becomes clear that having a stronger group-cohesion results in faster convergence times for the whole team in comparison to weaker or no group-cohesion. In case, where we would not want to use any group-cohesion, increasing the group size would actually worsen the last arrival times as shown in Fig. 16 where a comparison of CDFs concerning last arrival of group size $N = 5$ and $N = 30$ has been made.

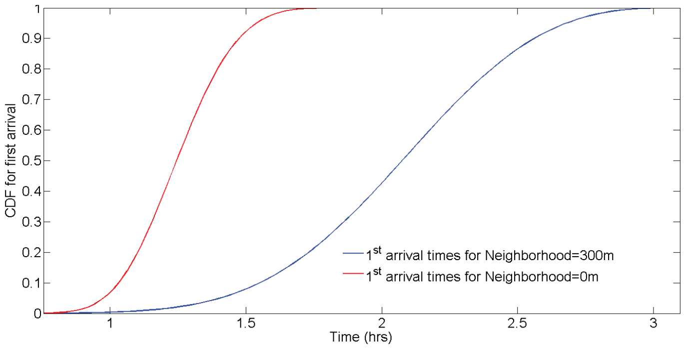

Fig. 11: CDF for first-arrival times for neighbourhood radii $r_\Psi \in \{0, 300\}$ for a group-size $N = 20$.

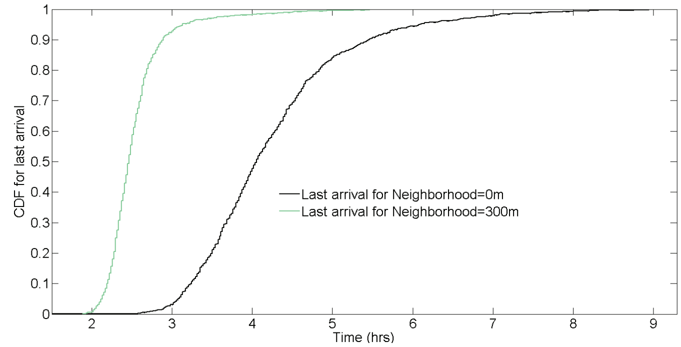

Fig. 14: CDF for last-arrival times for neighbourhood radii $r_\Psi \in \{0, 300\}$ for a group-size $N = 20$.

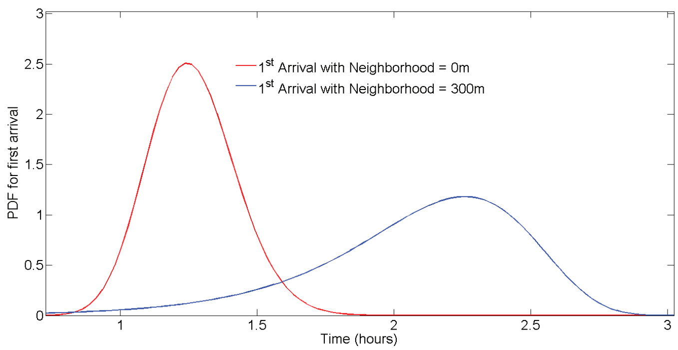

Fig. 12: PDF for first-arrival times for neighbourhood radii $r_\Psi \in \{0, 300\}$ for a group-size $N = 20$.

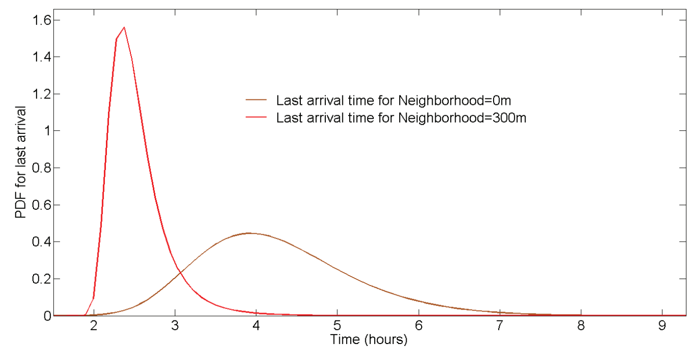

Fig. 15: PDF for last-arrival times for neighbourhood radii $r_\Psi \in \{0, 300\}$ for a group-size $N = 20$.

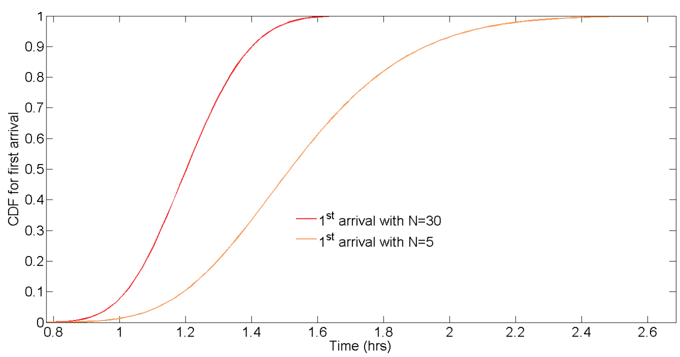

Fig. 13: CDF for first-arrival times for neighborhood radii $r_\Psi \in \{0\}$ and group-size $N = \{5, 30\}$.

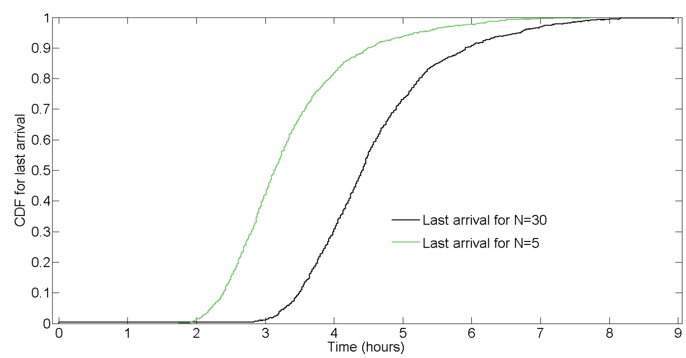

Fig. 16: CDF for last-arrival times for neighbourhood radii $r_\Psi \in \{0\}$ and group-size $N = \{5, 30\}$.

D. *Specific-arrival case*

Realizing such a constraint as given by Scenario 2 in Section II-A, where we have a particular AUV with additional capabilities which needs to reach the target location to mark the mission as a success; we need to find the probability of an arbitrary AUV within a group of N to reach the target location in a given amount of time. Fig. 17 and Fig. 18 refer to such a scenario where for a group size of $N = 20$ AUVs, comparison has been made between a group-cohesion case of $r_\Psi = 300$ m and no group-cohesion case of $r_\Psi = 0$ m. The results suggest that we can say with some level of certainty that the specialized vehicle will reach the target location in a period of 3 hours when the neighbourhood radius $r_\Psi = 300$ m. On the other hand, without any group-cohesion, it will take $t > 6$ hours to achieve the desired task. Hence, the group cohesion does play a significant role in case of a specific-arrival problem.

E. *'$\alpha > 1$' case*

Fig. 19 shows the average convergence response of a team of 20 AUVs where $\alpha = 1.2$ in (1) with varying levels of group cohesion. Results in Fig. 19 show the same trend as for $\alpha = 1$ in Fig. 4. What is more significant in the case of $\alpha > 1$ is the relative improvement in last-arrival times when a larger r_Ψ is used, compared to the case $\alpha = 1$.

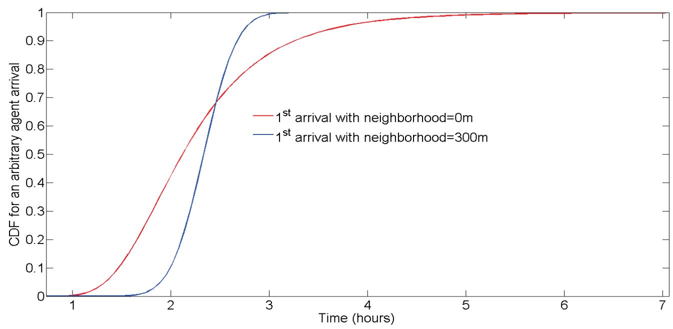

Fig. 17: CDF for robot arrival times for neighbourhood radii $r_\Psi \in \{0, 300\}$ for a group-size $N = 20$.

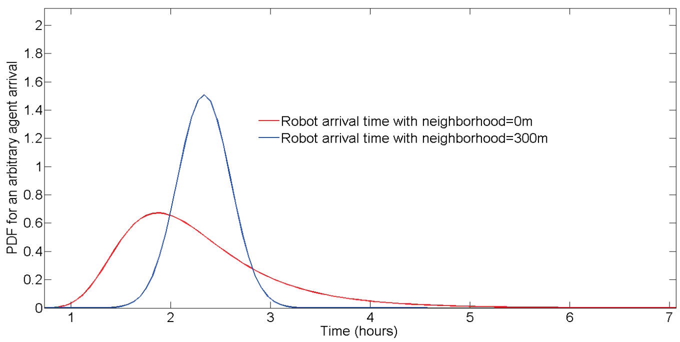

Fig. 18: PDF for robot arrival times for neighbourhood radii $r_\Psi \in \{0, 300\}$ for a group-size $N = 20$.

This suggests that group-cohesion plays a more significant role with its underlying concept of implicit averaging as α values increase and an individual AUV's decision-making becomes more prone to error.

V. Conclusion

We presented a novel bio-inspired algorithm for searching an underwater acoustic source in context of three different scenarios. The algorithm is a distributed infrastructure that only employs sensory data and does not depend on any explicit communications. This solves the major problem of coordinating an underwater team mission where communication methods are complex and hard to scale. The algorithm itself is a unified infrastructure derived from two different natural behaviours. Though inspiration has been drawn from natural swarms, the implementation of the algorithm is such that it preserves benefits of group cohesion even for very small teams. Detailed results have been presented which highlight the effect of varying neighbourhood-radius and group-size on the arrival times. For now, we have purposefully kept other algorithm parameters such as *cohesion-coefficient*, *drive-coefficient* and *sampling time* as constant. We can sum up our findings as follows:

1) There is a *dead-region* ($0 < r_\Psi \leq \phi_\Psi$) of neighbourhood radii for which there is no significant change in arrival times compared to the zero-neighbourhood response. ϕ_Ψ decreases with increasing neighbourhood radius and vice versa.

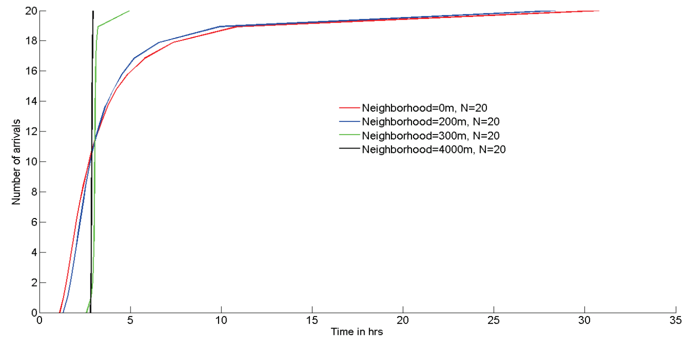

Fig. 19: Average arrival times over 1000 trials for varying neighbourhood sizes $r_\Psi \in \{0, 200, 300, 400\}$ for group size $N = 20$ and $\alpha = 1.2$.

2) To clock comparatively similar averaged arrival times, a larger group requires a smaller neighbourhood radius whereas a smaller group requires a larger neighbourhood radius.
3) There exists a limit $r_{\Psi_{max}}$ to which we can increase the neighbourhood radius to gain any significant advantage in terms of arrival times.
4) A *transition neighbourhood radius* $\acute{r}_\Psi$ has also been identified as a function of comparative group-sizes which acts as a threshold of swapping advantage either to employing a smaller or a larger group. This transition radius becomes important when we consider the practical constraints of a range measurement sensor.
5) In cases where first-arrival is of pivotal importance, we have shown that it is advantageous to keep the group-cohesion module inactivated. At the same time, first-arrival depends significantly on the group-size that we would employ. A larger group-size without any group-cohesion will guarantee a faster first-arrival.
6) In cases where we are more interested in the last-arrival, employing group-cohesion is beneficial. It has also been substantiated that larger group-size with group-cohesion and $\acute{r}_\Psi \leq r_\Psi \leq r_{\Psi_{max}}$ will ensure faster convergence for last-arrivals.
7) In cases where a specific AUV's arrival is more important, a larger neighbourhood radius when $r_\Psi \geq \acute{r}_\Psi$ will ensure a faster specific-arrival. Increasing the group size further reduces the arrival time.

VI. Future Work

The bio-inspired algorithm presented in this paper is a preliminary study which constitutes of a number of variable parameters and a set of assumptions. In future, one of the main emphasis would be to simplify and optimize the structure of the algorithm, and eliminate any redundant parameters. Some of the assumptions may also be relaxed to ensure that the simulation is in close agreement with the real world scenario.

In the presented work, we have kept ourselves to varying only group-size and neighbourhood-radius and investigating their role in influencing the arrival times. Two of the most important parameters of this algorithm are the cohesion-coefficient and the drive-coefficient, which if varied dynamically in some optimum way may improve the arrival times.

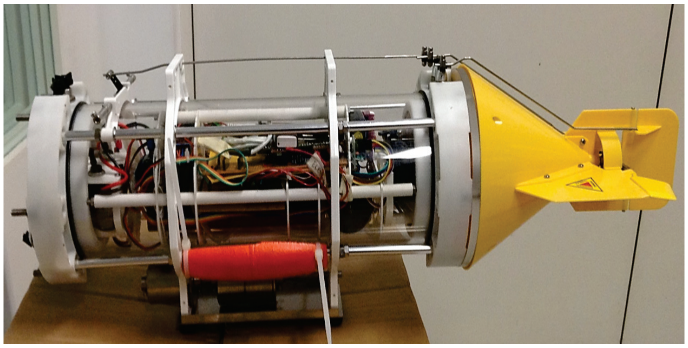

Fig. 20: SwarmBot is the smaller AUV being developed for future team-based operations.

Another critical mainstay of this algorithm is the 90-degree rule. We wish to investigate relaxing this rule so that based on actual conditions, AUV may choose the most optimum heading.

Apart from the on-going investigation pertaining to the algorithm parameters, we are also developing a flexible bio-inspired behavioural model that can accept different AUV models as input. This will enable us to gauge the approximate performance a particular team of AUVs may produce if programmed with this bio-inspired approach. This can be further extended to devising a unified infrastructure which can take an arbitrary bio-inspired model and an arbitrary AUV model as inputs and simulate the approximate scenario.

The real test of the performance of any algorithm is in the real-world. Currently, the number of STARFISH AUVs [55] we have developed at our lab, is not sufficient to give us any meaningful real-world analysis of the presented algorithm. To address this problem, we are developing a miniature version AUV known as SwarmBot for lake deployment. SwarmBot as shown in Fig. 20 will be a low-cost solution with minimum on-board sensors. This will give us a test-bed to gauge real-world performance of the algorithm for a small team of AUVs.

REFERENCES

[1] L. Nana, F. Singhoff, J. Legrand, J. Vareille, P. Le Parc, F. Monin, D. Masse, L. Marce, J. Opderbecke, M. Perrier, and V. Rigaud, "Embedded intelligent supervision and piloting for oceanographic auv," in *Oceans 2005*, vol. 2, june 2005, pp. 889 – 895 Vol. 2.

[2] D. A. Smale, G. A. Kendrick, and Harvey, "Regional-scale benthic monitoring for ecosystem-based fisheries management (ebfm) using an autonomous underwater vehicle (auv)," *ICES Journal of Marine Science: Journal du Conseil*, 2012. [Online]. Available: http://icesjms.oxfordjournals.org/content/early/2012/05/18/icesjms.fss082.abstract

[3] N. Barrett, J. Seiler, T. Anderson, S. Williams, S. Nichol, and S. Hill, "Autonomous underwater vehicle (auv) for mapping marine biodiversity in coastal and shelf waters: Implications for marine management," in *OCEANS 2010 IEEE - Sydney*, may 2010, pp. 1 –6.

[4] J. Nicholson and A. Healey, "The present state of autonomous underwater vehicle (auv) applications and technologies," *Marine Technology Society Journal*, vol. 42, no. 1, pp. 44–51, 2008. [Online]. Available: http://www.ingentaconnect.com/content/mts/mtsj/2008/00000042/00000001/art00008

[5] R. Marthiniussen, K. Vestgard, R. Klepaker, and N. Storkersen, "Hugin-auv concept and operational experiences to date," *OCEANS '04. MTTS/IEEE TECHNO-OCEAN '04*, vol. 2, pp. 846 – 850 Vol.2, nov. 2004.

[6] R. Prins and M. Kandemir, "Time-constrained optimization of multi-auv cooperative mine detection," in *OCEANS 2008*, sept. 2008, pp. 1 –13.

[7] E. Fiorelli, N. E. Leonard, P. Bhatta, D. A. Paley, R. Bachmayer, and D. M. Fratantoni, "Multi-auv control and adaptive sampling in monterey bay," *Oceanic Engineering, IEEE Journal of*, vol. 31, no. 4, pp. 935 –948, oct. 2006.

[8] D. Pompili and I. Akyildiz, "Overview of networking protocols for underwater wireless communications," *Communications Magazine, IEEE*, vol. 47, no. 1, pp. 97 –102, january 2009.

[9] M. Chitre, S. Shahabudeen, and M. Stojanovic, "Underwater acoustic communications and networking: Recent advances and future challenges," *Oceanic Engineering, IEEE Journal of*, pp. 103 –116, spring 2008.

[10] M. Stojanovic and J. Preisig, "Underwater acoustic communication channels: Propagation models and statistical characterization," *Communications Magazine, IEEE*, vol. 47, no. 1, pp. 84 –89, january 2009.

[11] M. Stojanovic, "Acoustic (underwater) communications," *Encyclopedia of Telecommunications*, 2003.

[12] ——, "On the relationship between capacity and distance in an underwater acoustic communication channel," in *Proceedings of the 1st ACM international workshop on Underwater networks*, ser. WUWNet '06. New York, NY, USA: ACM, 2006, pp. 41–47. [Online]. Available: http://doi.acm.org/10.1145/1161039.1161049

[13] ——, "Underwater wireless communications: Current achievements and research challenges," *IEEE Oceanic Engineering Society Newsletter*, 2006.

[14] J.-H. Cui, J. Kong, M. Gerla, and S. Zhou, "The challenges of building mobile underwater wireless networks for aquatic applications," *Network, IEEE*, vol. 20, no. 3, pp. 12 – 18, may-june 2006.

[15] J. C. Barca and Y. A. Sekercioglu, "Swarm robotics reviewed," *Robotica*, vol. FirstView, pp. 1–15, 2012. [Online]. Available: http://dx.doi.org/10.1017/S026357471200032X

[16] B. Anderson, C. Yu, B. Fidan, and J. Hendrickx, "Rigid graph control architectures for autonomous formations," *Control Systems, IEEE*, vol. 28, no. 6, pp. 48–63, 2008.

[17] D. Hart and P. Craig-Hart, "Reducing swarming theory to practice for uav control," in *Aerospace Conference, 2004. Proceedings. 2004 IEEE*, vol. 5. IEEE, 2004, pp. 3050–3063.

[18] P. Vincent and I. Rubin, "A framework and analysis for cooperative search using uav swarms," in *Proceedings of the 2004 ACM symposium on Applied computing*. ACM, 2004, pp. 79–86.

[19] S. Edwards, *Swarming on the Battlefield: past, Present, and Future*. Rand Corporation, 2000.

[20] J. Cortes, S. Martinez, T. Karatas, and F. Bullo, "Coverage control for mobile sensing networks," *Robotics and Automation, IEEE Transactions on*, vol. 20, no. 2, pp. 243–255, 2004.

[21] J. Pugh and A. Martinoli, "Distributed adaptation in multi-robot search using particle swarm optimization," *From Animals to Animats 10*, pp. 393–402, 2008.

[22] K. Lerman, A. Martinoli, and A. Galstyan, "A review of probabilistic macroscopic models for swarm robotic systems," *Swarm robotics*, pp. 143–152, 2005.

[23] Y. Cao, A. Fukunaga, and A. Kahng, "Cooperative mobile robotics: Antecedents and directions," *Autonomous robots*, vol. 4, no. 1, pp. 7–27, 1997.

[24] J. Barca, G. Rumantir, and R. Li, "A concept for optimizing behavioural effectiveness & efficiency," *Intelligent Engineering Systems and Computational Cybernetics*, pp. 449–458, 2009.

[25] M. Chitre, "Teamwork among marine robots–advances and challenges," *Workshop on Marine Robotics*, 2013.

[26] S. Bazazi, J. Buhl, J. Hale, M. Anstey, G. Sword, S. Simpson, and I. Couzin, "Collective motion and cannibalism in locust migratory bands," *Current Biology*, vol. 18, no. 10, pp. 735–739, 2008.

[27] I. Bajec and F. Heppner, "Organized flight in birds," *Animal Behaviour*, vol. 78, no. 4, pp. 777–789, 2009.

[28] J. Pearce-Duvet, C. Elemans, and D. Feener, "Walking the line: search behavior and foraging success in ant species," *Behavioral Ecology*, vol. 22, no. 3, pp. 501–509, 2011.

[29] A. Magurran and A. Higham, “Information transfer across fish shoals under predator threat,” *Ethology*, vol. 78, no. 2, pp. 153–158, 2010.

[30] M. LARSSON, “Why do fish school?” *Current Zoology*, vol. 58, 2012.

[31] T. Seeley, P. Visscher, T. Schlegel, P. Hogan, N. Franks, and J. Marshall, “Stop signals provide cross inhibition in collective decision-making by honeybee swarms,” *Science*, vol. 335, no. 6064, pp. 108–111, 2012.

[32] T. Balch and R. Arkin, “Communication in reactive multiagent robotic systems,” *Autonomous Robots*, vol. 1, no. 1, pp. 27–52, 1994.

[33] D. Sumpter, *Collective animal behavior*. Princeton University Press, 2010.

[34] R. Beckers, O. Holland, and J.-L. Deneubourg, “From local actions to global tasks: Stigmergy and collective robotics,” in *Artificial life IV*, vol. 181, 1994, p. 189.

[35] D. Payton, R. Estkowski, and M. Howard, “Compound behaviors in pheromone robotics,” *Robotics and Autonomous Systems*, vol. 44, no. 3, pp. 229–240, 2003.

[36] A. Sharkey, “Robots, insects and swarm intelligence,” *Artificial Intelligence Review*, vol. 26, no. 4, pp. 255–268, 2006.

[37] R. Cazangi, F. Von Zuben, and M. Figueiredo, “Autonomous navigation system applied to collective robotics with ant-inspired communication,” in *Proceedings of the 2005 conference on Genetic and evolutionary computation*. ACM, 2005, pp. 121–128.

[38] G. Ferri, E. Caselli, V. Mattoli, A. Mondini, B. Mazzolai, and P. Dario, “Spiral: A novel biologically-inspired algorithm for gas/odor source localization in an indoor environment with no strong airflow,” *Robotics and Autonomous Systems*, vol. 57, no. 4, pp. 393–402, 2009.

[39] A. Lilienthal, D. Reiman, and A. Zell, “Gas source tracing with a mobile robot using an adapted moth strategy,” *Autonome Mobile Systeme (AMS), 18. Fachgespräch*, pp. 150–160, 2003.

[40] J. A. Farrell, S. Pang, W. Li, and R. Arrieta, “Chemical plume tracing experimental results with a remus auv,” in *OCEANS 2003. Proceedings*, vol. 2. IEEE, 2003, pp. 962–968.

[41] W. Li, J. Farrell, S. Pang, and R. Arrieta, “Moth-inspired chemical plume tracing on an autonomous underwater vehicle,” *Robotics, IEEE Transactions on*, vol. 22, no. 2, pp. 292–307, 2006.

[42] F. Li, Q.-H. Meng, S. Bai, J.-G. Li, and D. Popescu, “Probability-pso algorithm for multi-robot based odor source localization in ventilated indoor environments,” *Intelligent Robotics and Applications*, pp. 1206–1215, 2008.

[43] L. Marques, U. Nunes, and A. De Almeida, “Particle swarm-based olfactory guided search,” *Autonomous Robots*, vol. 20, no. 3, pp. 277–287, 2006.

[44] A. Marjovi, J. Nunes, P. Sousa, R. Faria, and L. Marques, “An olfactory-based robot swarm navigation method,” in *Robotics and Automation (ICRA), 2010 IEEE International Conference on*. IEEE, 2010, pp. 4958–4963.

[45] C. Zhang, D. Arnold, N. Ghods, A. Siranosian, and M. Krstic, “Source seeking with non-holonomic unicycle without position measurement and with tuning of forward velocity,” *Systems & control letters*, vol. 56, no. 3, pp. 245–252, 2007.

[46] C. Zhang, A. Siranosian, and M. Krstić, “Extremum seeking for moderately unstable systems and for autonomous vehicle target tracking without position measurements,” *Automatica*, vol. 43, no. 10, pp. 1832–1839, 2007.

[47] J. Vaganay, P. Baccou, and B. Jouvencel, “Homing by acoustic ranging to a single beacon,” in *OCEANS 2000 MTS/IEEE Conference and Exhibition*, vol. 2. IEEE, 2000, pp. 1457–1462.

[48] P. Baccou and B. Jouvencel, “Homing and navigation using one transponder for auv, postprocessing comparisons results with long base-line navigation,” in *Robotics and Automation, 2002. Proceedings. ICRA’02. IEEE International Conference on*, vol. 4. IEEE, 2002, pp. 4004–4009.

[49] F. Bezruchko, I. Burdinsky, and A. Myagotin, “Global extremum searching algorithm for the auv guidance toward an acoustic buoy,” in *OCEANS, 2011 IEEE-Spain*. IEEE, 2011, pp. 1–7.

[50] C. Radford, J. Stanley, S. Simpson, and A. Jeffs, “Juvenile coral reef fish use sound to locate habitats,” *Coral Reefs*, vol. 30, no. 2, pp. 295–305, 2011.

[51] J. Potter and M. Chitre, “Do fish fry use emergent behaviour in schools to find coral reefs by sound,” in *AGU Ocean Sciences Meeting, Honolulu, Hawaii*, 2006.

[52] S. Simpson, M. Meekan, J. Montgomery, R. McCauley, and A. Jeffs, “Homeward sound,” *Science*, vol. 308, no. 5719, pp. 221–221, 2005.

[53] Y. Katz, K. Tunstrøm, C. Ioannou, C. Huepe, and I. Couzin, “Inferring the structure and dynamics of interactions in schooling fish,” *Proceedings of the National Academy of Sciences*, vol. 108, no. 46, pp. 18 720–18 725, 2011.

[54] J. C. Montgomery, A. Jeffs, S. D. Simpson, M. Meekan, and C. Tindle, “Sound as an orientation cue for the pelagic larvae of reef fishes and decapod crustaceans,” *Advances in marine biology*, vol. 51, pp. 143–196, 2006.

[55] T. Koay, Y. Tan, Y. Eng, R. Gao, M. Chitre, J. Chew, N. Chandhavarkar, R. Khan, T. Taher, and J. Koh, “Starfish–a small team of autonomous robotic fish,” *Indian Journal of Geo-Marine Sciences*, vol. 40, no. 2, pp. 157–167, 2011.